Assessing Biodegradability and Mechanical, Thermal, and Morphological Properties of an Acrylic Acid-Modified Poly(3-hydroxybutyric acid)/Wood Flours Biocomposite

Chin-San Wu

Department of Biochemical Engineering and Graduate Institute of Environmental Polymer Materials, Kao Yuan University, Kaohsiung County, Taiwan 82101, Republic of China

Received 13 December 2005; accepted 15 May 2005
DOI 10.1002/app.24817
Published online in Wiley InterScience (www.interscience.wiley.com).

ABSTRACT: A poly(3-hydroxybutyric acid) and wood flours (PHB/wood flours) composite and an acrylic acid-grafted PHB/wood flours composite were characterized and their properties were examined and compared. Mechanical properties of PHB became significantly worse when it was blended with wood flours, due to the poor compatibility between the two phases. Much better dispersion and homogeneity of wood flours in the polymer matrix was obtained when PHB-*g*-acrylic acid (AA) was used in place of PHB in the composite. Improved mechanical and thermal properties of the PHB-*g*-AA/wood flours composite, notably an increase in tensile strength at breakpoint, evidenced its superiority to the PHB/wood flours composite. Furthermore, PHB-*g*-AA/wood flours composites were more easily processed because of their lower melt viscosity. Under soil and enzymatic environments, weight loss data indicated that both composites were more biodegradable with higher wood flours content. A reduction in tensile strength at break after exposure to soil and enzymatic environments was also observed in both blends, especially at high wood flours content. © 2006 Wiley Periodicals, Inc. J Appl Polym Sci 102: 3565–3574, 2006

Key words: biodegradation; poly(3-hydroxybutyric acid); wood flours; biocomposite

INTRODUCTION

In response to increased awareness of the environmental hazards associated with disused plastics, much research is focused on producing biodegradable plastics/materials. One such material is poly-3-hydroxybutyrate (PHB), which is 100% biodegradable (after a few weeks in soil and other environments) and can be produced from renewable resources. Moreover, with physical properties similar to polypropylene, PHB has attracted much attention as an alternative plastic for a wide range of agricultural, marine, and medical applications. Its use at present, however, is restricted mainly to medical applications because of its high cost compared to synthetic plastics. Methods aimed at reducing the cost of production of PHB include the development of better bacterial strains and more efficient fermentation/recovery processes, and the use of low cost renewable resources as substrates. Some attempts have also been made to improve the physical properties of PHB by blending it with other biodegradable polymers found to be miscible with PHB, such as polyethylene oxide,[1] cellulose esters,[2] and starch.[3] Wood flours (WFs), being abundant, cheaply available, and able to blend with PHB to form favorably biodegradable material, are particularly good candidates for obtaining desired physical properties with concomitant reduction in cost. Additionally, compared with mineral or inorganic fillers, they have low density, flexibility during processing with no harm to equipment, and acceptable specific strength properties.

In spite of the environmental and economic advantages over traditional mineral or inorganic fillers, wood-based fillers such as WFs are not popular components of thermoplastic composites. One reason is the reported poor mechanical properties of composites containing WFs, caused by poor adhesion of the hydrophilic WFs and the hydrophobic synthetic polymer. However, a reactive functional group introduced into the synthetic polymer as compatibilizer and toughener can enhance the compatibility between the two immiscible polymers and hence improve the mechanical properties of the blend.[4,5] Styrene–butadiene–styrene block copolymer was shown to be an effective compatibilizer in a polyethylene/wood flours (PE/WFs) composite.[6] Meanwhile, a maleated polypropylene effectively increased compatibility of a polypropylene/cellulose fiber (PP/CF) composite.[7]

In this article, we will systematically investigate the effect of replacing pure PHB with acrylic acid-grafted PHB (PHB-*g*-AA), synthesized in our laboratory, on the structure and properties of PHB/WFs composites. Similar investigations have shown that

Correspondence to: C.-S. Wu (cws1222@cc.kyu.edu.tw).

higher amounts of starch (up to 20–30 wt %) can be incorporated into polymers.[7,8] In this work, therefore, we will add WFs up to 50 wt % to find an optimal content. Fourier transform infrared (FTIR) spectroscopy and nuclear magnetic resonance (NMR) are used to characterize the composites, while XRD spectroscopy and differential scanning calorimetry (DSC) are applied to understand the structural change that occurs in the acrylic acid-grafted PHB. Additionally, scanning electron microscopy (SEM) is used to examine morphology and an Instron mechanical tester used to examine mechanical properties of the blends. Furthermore, water absorption of blends and weight loss of buried blends were estimated to assess water resistance and biodegradability, respectively.

EXPERIMENTAL PART

Materials

Poly(3-hydroxybutyric acid), molecular weight (M_w) 7.72×10^5, molecular weight number (M_n) 5.25×10^5, polydisperity index 1.47, intrinsic viscosity $[\eta] = (\eta_{sp}/c)_{c=0}$ 3.16 dL/g, and melt-flow index 22.6 g/10 min, was used as supplied by Aldrich Chemical (Milwaukee, WI). Also supplied by Aldrich, acrylic acid was purified by recrystallization from chloroform before use, and benzoyl peroxide (BPO), used as an initiator, was purified by dissolution in chloroform and reprecipitation with methanol. *p*-Cresol and α-amylase (reported by the manufacturer to have a specific activity of 130 U/mg) were obtained from Sigma and Merck Chemical. The WFs, ''Celluflex,'' supplied by Zell Wildshausen GMBH (Steinheim, Germany), had a grain size of 100% finer than 250 μm, 87% finer than 100 μm and 37% finer than 50 μm. The moisture content of the WFs was (8 ± 2)% and the apparent density was 0.10–0.12 g/cm^3. PHB-*g*-AA, constructed in our laboratory according to procedures described in our previous work,[9] had a M_w of 7.16×10^5, a M_n of 4.53×10^5, a polydisperity index of 1.58, an η of 3.03 dL/g, and a melt-flow index of 23.8 g/10 min. As the grafting percentage of PHB-*g*-AA was only about 5.75 wt %, the structure of PHB-*g*-AA was not noticeably different to that of PHB, and the physical properties varied only slightly. Nevertheless, a slight decrease in molecular weight and intrinsic viscosity and a slight increase in melt-flow index were apparent in PHB-*g*-AA, due to some degradation of the bond in the grafting reaction.

Sample preparation

Grafting reaction and sample preparation

A mixture of AA and BPO was added in four equal portions at 2-min intervals to the solution of PHB in xylene to allow grafting reaction to take place. The reaction was carried out under nitrogen at (85 ± 2)°C. Preliminary experiments showed that reaction equilibrium was attained in less than 6 h, and reactions were therefore allowed to progress for 6 h, at a rotor speed of 60 rpm. The product (4 g) was dissolved in 200 mL of refluxing xylene at 85°C and the solution was then filtered through several layers of cheesecloth. The xylene-insoluble product remaining on the cheesecloth was washed using acetone to remove the unreacted acrylic acid and was then dried in a vacuum oven at 80°C for 24 h. The xylene-soluble product in the filtrate was extracted five times, using 600 mL of cold acetone for each extraction. Using a titration method,[10] percentage grafting was determined to be about 5.75 wt % with BPO loading and AA loading at 0.3 and 10 wt %, respectively.

Composite preparation

The composites were prepared using a Brabender ''Plastograph'' 200Nm mixer W50EHT instrument with a blade-type rotor, with rotor speed maintained at 50 rpm and blending temperature at 190°C, and a reaction time of 15 min. The WFs were dried in an oven at 105°C for 24 h prior to blending. Mass ratios of WFs to PHB were fixed at 10/90, 20/80, 30/70, 40/60, and 50/50. After blending, the composites were pressed into thin plates using a hot press at 190°C, and the plates put into a dryer, relative humidity (50 ± 5)%, for cooling/conditioning for 24 h. It was found that 24 h of conditioning is sufficient for dehydrating samples to appropriate water content and that conditioning times in excess of this had no further appreciable effect on the properties of composites.

Characterization of composites

NMR/FTIR/XRD/DSC analyses of PHB and PHB-*g*-AA

To characterize the composites, solid-state ^{13}C NMR analysis was performed using a Bruker AMX 400 ^{13}C NMR spectrometer at conditions of 50 MHz, and spectra were observed under cross-polarization, magic antic angle sample spinning and power decoupling conditions with 90° pulse and 4 s cycle time. Additionally, infrared spectra of samples were obtained using a Bio-Rad FTS-7PC type FTIR spectrophotometer.

To enable changes in the crystal structure to be studied, X-ray diffraction intensity spectra, recorded using a Rigaku D/max 3V X-ray diffractometer with a Cu target and Kα radiation at a scanning rate of 2°/min, were obtained. Furthermore, the melting temperature (T_m) and enthalpy of melting (ΔH_m)

were determined using a TA instrument 2010 DSC system. For the DSC tests, sample amounts were between 4 and 6 mg, and the melting curves were recorded from −30 to +120°C, heated at a rate of 10°C/min.

Mechanical properties

Following the ASTM D638-04 method, an Instron mechanical tester (Model Lloyd, LR5K type) was used to measure the tensile strength at breakpoint of all blends. Five thin plates (about 1 mm thickness) were tested for each blend at a 20 mm/min crosshead speed, and a mean value was subsequently calculated for the blend.

Composite morphology

Subsequent to mechanical analysis, the plates were treated with hot water at 80°C for 24 h. Then the samples were coated with gold and their morphology was examined using a Hitachi Microscopy Model S-1400 scanning electron microscope.

Water absorption

Samples for assessing water absorption were in the form of 75 × 25 mm^2 strips of 150 ± 5 μm thickness, following the ASTM D570-81 method. The samples (five in total) were dried in a vacuum oven at (50 ± 2)°C for 8 h, cooled in a desiccator, and then immediately weighed to the nearest 0.001 g (this weight designated as W_c). The conditioned samples were then immersed in distilled water, maintained at (25 ± 2)°C, for a 6-week test period. During this period, they were removed from the water at 1-week intervals, gently blotted with tissue paper to remove excess water on the surface, immediately weighed to the nearest 0.001 g (three times to ensure against erroneous measurements), and returned to the water. The average value obtained from the three measurements was designated W_w. The percentage increase of water (in weight) was calculated to the nearest 0.01% as follows:

$$\% W_f = \frac{W_w - W_c}{W_c} \times 100$$

where W_f is the final percentage increase in weight of the tested samples.

Biodegradation studies

Biodegradability of the samples was assessed by evaluating weight loss of blends over time in (1) a soil environment and (2) an enzymatic environment.

Exposure to soil environment. Five samples of (30 mm × 30 mm × 1 mm) were weighed and then buried in boxes of alluvial-type soil, obtained in May 2005 from farmland topsoil before planting. The soil was sifted to remove large clumps and plant debris. Procedures used for soil burial were as those described by Wu.[11] Soil was maintained at ∼ 20% moisture in weight and samples were buried at a depth of 15 cm, following the ASTM D6954-04. A control box consisted of only samples and no soil. The buried samples were removed from the soil once a week, washed in distilled water, dried in a vacuum oven at (50 ± 2)°C for 24 h and equilibrated in a desiccator for at least a day, before being weighed and then returned to the soil.

Exposure to enzymatic environment. Also, five samples in total of size 50 mm × 50 mm × 1 mm were cast using a plastic mold. These samples were washed with a large quantity of distilled water several times until the water was neutral. They were then dried, first while clamped to a piece of glass and subsequently in a vacuum oven [(50 ± 2)°C, 0.5 mmHg, 24 h], producing 0.05 ± 0.02 mm thick films. The films were exposed to an enzymatic environment of 30 mL phosphate buffer (100 m*M*; pH 6.3) containing *p*-cresol (1.8 m*M*) and α-amylase (20 U/mL), incubated in compost petri dishes at (30 ± 2)°C and (50 ± 5)% relative humidity. After reaction, they were washed extensively with deionized water and then dried.

The studies were conducted using three replicate test reactors and three replicate samples in each test reactor for each exposure time, giving nine samples for each exposure time. There was also a poisoned vessel, maintained under the same conditions as the bioactive test reactors, which served as an α-amylase control.

RESULTS AND DISCUSSION

Characterization of PHB-*g*-AA/WFs

FTIR spectroscopy and ^{13}C NMR were used in this study to investigate the grafting of acrylic acid onto PHB. FTIR spectroscopic analysis of both unmodified PHB and PHB-*g*-AA produced spectra [Figs. 1(A) and 1(B), respectively] with the characteristic peaks of PHB (at 3300–3700, 1700–1750, and 500–1500 cm^{-1}).[12,13] The spectrum of modified PHB, however, contains an extra peak at 1710 cm^{-1}, characteristic of —C=O, and a broad O=H stretching absorbance at 3200–3700 cm^{-1} [Fig. 1(B)]. Similar results have been reported elsewhere.[14,15] The discernible shoulder near 1710 cm^{-1} is a product of free acid from the modified polymer, demonstrating that acrylic acid had been grafted onto PHB. Furthermore, compared with PHB and PHB-*g*-AA, the

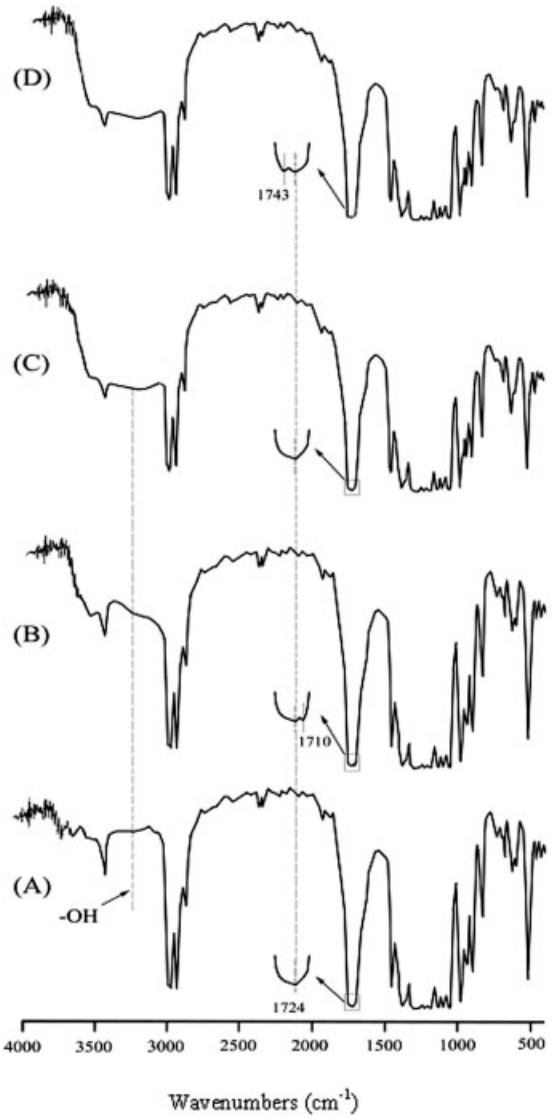

Figure 1 FTIR spectra of pure PHB and composites. (A): pure PHB; (B): PHB-*g*-AA; (C): PHB/WFs (30 wt %); (D): PHB-*g*-AA/WFs (30 wt %).

FTIR spectrum of PHB/WFs (30 wt %), shown in Figure 1(C), has a much more intense peak assigned to the O—H bond stretching vibration at 3200–3700 cm^{-1}, due to the extra contribution from the —OH group of WFs.[5,16] The spectra of PHB/WFs (30 wt %) and PHB-*g*-AA/WFs (30 wt %), shown in Figures 1(C) and 1(D), respectively, differ in respect to an absorption peak at 1743 cm^{-1} in the latter, assigned to ester carbonyl stretching vibration in the copolymer. This is supported by the study of Oksman and Clemons,[17] in which the FTIR spectrum of ester carbonyl showed its absorption peak at 1746 cm^{-1}. Expansion of the FTIR spectra in the limited range 1700–1750 cm^{-1} more clearly illustrates the difference between PHB/WFs and PHB-*g*-AA/WFs, as it highlights the peak at 1743 cm^{-1} in the latter and the broad absorption band at 1720–1750 cm^{-1} in the former. This absorption band, also present in PHB at 1700–1750 cm^{-1}, is representative of —C=O stretching vibration. Based on the above result, one can infer that branched macromolecules may be produced in PHB-*g*-AA/WFs as a result of interaction between the carboxyl groups of the copolymer and the hydroxyl groups of WFs.

The ^{13}C NMR spectrum of PHB [Fig. 2(A)] shows carbon peaks in four places for unmodified PHB (1: $\delta = 170.06$ ppm; 2: $\delta = 40.96$ ppm; 3: $\delta = 67.46$ ppm; 4: $\delta = 19.96$ ppm). Doi et al.[18] reported a similar outcome in their study of 3-hydroxybutyrate and 4-hydroxybutyrate copolyesters. Additional peaks (C_β: $\delta = 35.63$ ppm; a: $\delta = 175.05$ ppm) seen in the ^{13}C NMR spectrum of PHB-*g*-AA [Fig. 2(B)] confirm that AA had grafted onto PHB. A third additional peak (C_α: $\delta = 42.19$ ppm) should be observed but, because the amount of grafted AA is small, this is overlapped by peak 2 of PHB. All three peaks were observed in a previous work, a ^{13}C NMR analysis of POE-*g*-AA,[14] and it was indicated in that work that these peaks were caused by grafting of AA onto POE.

Figure 3 shows the ^{13}C NMR spectra of PHB-*g*-AA/WFs, PHB/WFs, and WFs. The spectra correspond with those reported elsewhere.[19] Moreover, a comparison of PHB-*g*-AA/WFs [Fig. 3(A)] and PHB/WFs [Fig. 3(B)] reveals additional peaks at $\delta = 35.6$ ppm (C_β), $\delta = 176.9$ ppm (b), and $\delta = 178.3$ ppm (c) in the latter. It was found that the peak at "a" ($\delta = 175.05$ ppm) in the spectrum of PHB-*g*-AA [Fig. 2(B)] was absent in PHB-*g*-AA/WFs [Fig. 3(A)]. This

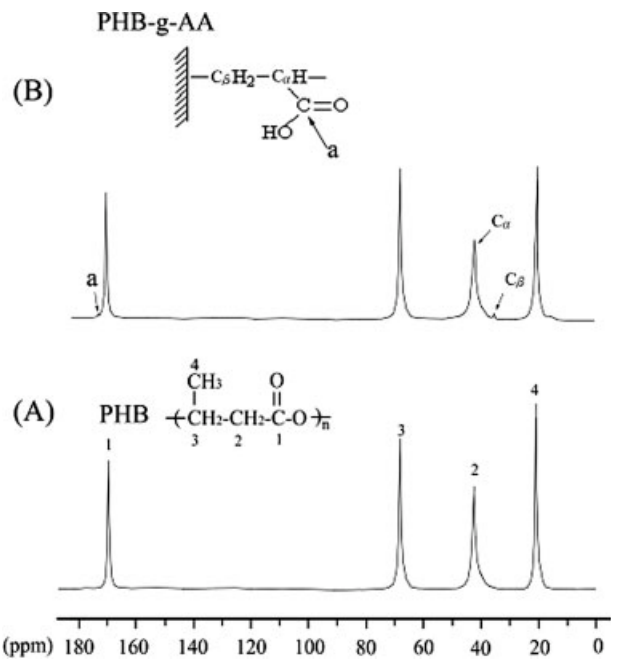

Figure 2 ^{13}C NMR spectra of pure PHB and PHB-*g*-AA.

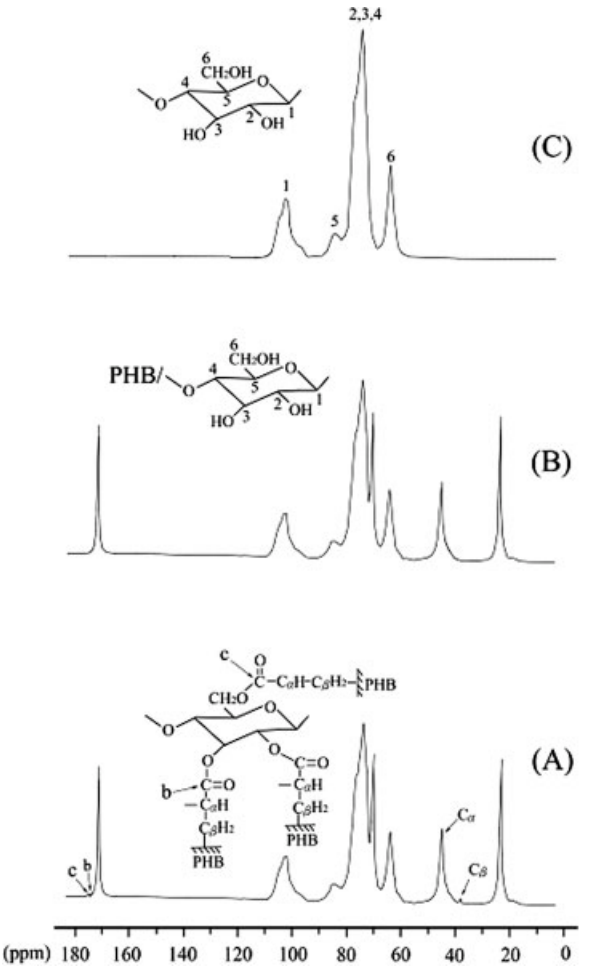

Figure 3 ^{13}C NMR spectra of pure PHB and composites. (A): PHB-*g*-AA/WFs (30 wt %); (B): PHB/WFs (30 wt %); (C): WFs.

is because the reaction between —COOH of AA and —OH of WFs shifts the peak at ''a'' to the duplicates at ''b'' and ''c.'' This provides further evidence of the condensation between PHB-*g*-AA and WFs, and leads to the conclusion that the original WFs were fully —OH, and that in this reaction the $-CH_2OH$ and —OH groups of WFs were converted to $-\overset{O}{\overset{\|}{C}}=O$ (represented by peaks ''b'' and ''c''). Conversely, there is no evidence of reaction between PHB and WFs because no corresponding peaks were observed in Figure 3(B). Formation of ester functional groups has a profound effect on structure, thermal, and mechanical properties, and biodegradation, something that will be discussed in the following sections.

X-ray diffraction

The XRD spectra of pure PHB, PHB/WFs (30 wt %) composite, and PHB-*g*-AA/WFs (30 wt %) composite are shown in Figures 4(A)–4(C), respectively. Showing similarity to the results of Galego et al.,[20] pure PHB produced seven peaks at about 13.1°, 16.9°, 19.6°, 21.3°, 22.5°, 25.6°, and 27.1°. Two additional peaks were observed for the PHB/WFs composite, at about 17.1° and 15.0°. These peaks may be due to the change in coordinate property of PHB molecules when WFs were blended with it,[21,22] suggesting that WFs were dispersed physically in the PHB matrix. Moreover, it also implies that the secondary valance force is more predominant in blends.

Figure 4(C) shows a new peak at 18.1° for the PHB-*g*-AA/WFs composite. This new peak, also identified by Shogren et al.,[23] may be caused by the formation of an ester carbonyl group, as described in the FTIR and NMR spectra analysis, and provides evidence that the crystalline structure of the PHB/WFs composite is altered when PHB-*g*-AA is used in it.

Torque measurements

The results of torque versus mixing time for PHB/WFs and PHB-*g*-AA/WFs blends are presented in

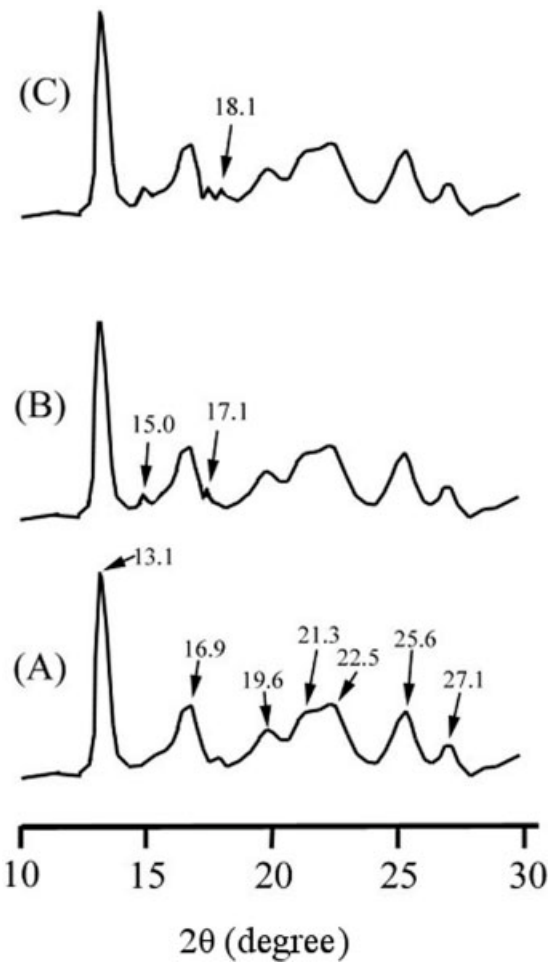

Figure 4 X-ray diffraction spectra of pure PHB and composites. (A): pure PHB; (B): PHB/WFs (30 wt %); (C): PHB-*g*-AA/WFs (30 wt %).

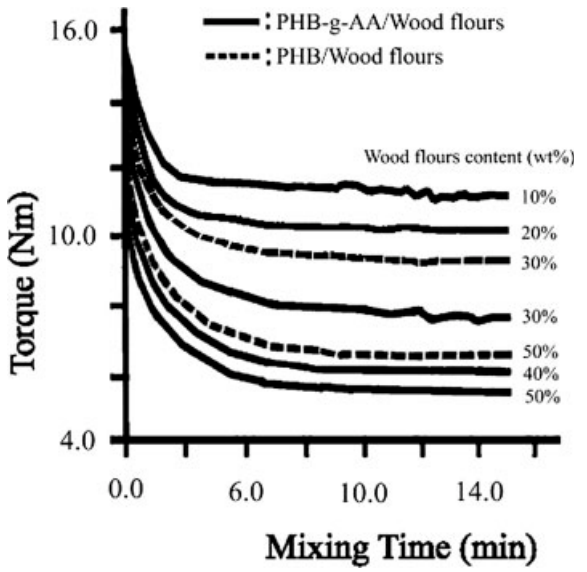

Figure 5 Torque values versus mixing time for PHB/WFs and PHB-*g*-AA/WFs blends at various WFs contents.

Figure 5. The torque value of both blends decreased with increasing WFs content and mixing time, and approached a stable value when the mixing time was greater than 8 min, suggesting that good mixing had occurred after this time. Final torque decreased with increasing WFs content because the viscosity of molten WFs is lower than that of molten PHB or PHB-*g*-AA. Furthermore, the torque response of PHB-*g*-AA/WFs was significantly lower than that of PHB/WFs at the same WFs content (30 and 50 wt %). The improved rheological behavior of PHB-*g*-AA/WFs is attributed to the conformational change of the WFs molecule,[24] caused by the previously discussed formation of an ester carbonyl functional group. Liao and Wu[16] reported that the melt viscosity of esterified WFs also decreased with increasing molecular weight of the ester group. Another possible cause is that WFs behave as filler within the molten PHB matrix. The main contribution for the torque value is from the molten PHB. As the WFs content increases, expansion and stretch of PHB/WFs and PHB-*g*-AA/WFs matrices also increases, making movement of molten PHB or PHB-*g*-AA easier at higher WFs contents, and resulting in the decrease in torque.

Differential scanning calorimetry analysis

Thermal properties of pure PHB, PHB/WFs, and PHB-*g*-AA/WFs, obtained via DSC, are given in Figures 6 and 7. The melting temperature (T_m) and fusion heat (ΔH_m) of pure PHB were 173.1°C and 78.5 J/g, respectively. With increased WFs content, the T_m and ΔH_m decreased for both PHB/WFs and PHB-*g*-AA/WFs. The decrease in T_m is due to the lower melt viscosity of WFs compared to that of PHB

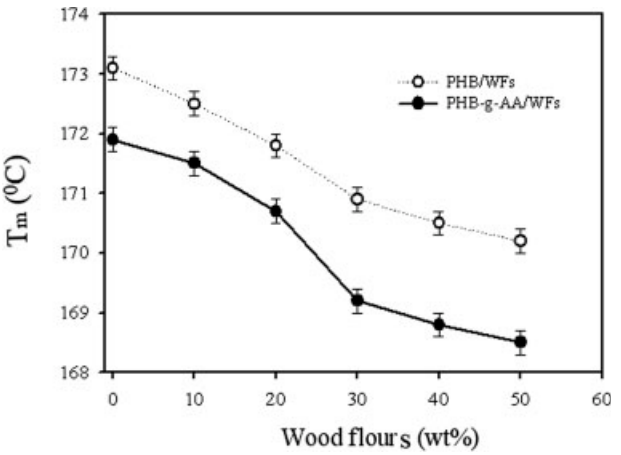

Figure 6 Melting temperature versus WFs content for PHB/WFs and PHB-*g*-AA/WFs blends.

or PHB-*g*-AA.[25] On the other hand, the decrease in crystallization was probably caused by the increased difficulty in arranging the polymer chain, due to WFs prohibiting movement of the polymer segments. Another potential cause is the hydrophilic character of WFs, which would lead to poor adhesion with the hydrophobic PHB. Liao and Wu,[16] who studied the properties of WFs blended with polyethylene-octene elastomer, reported similar phenomena. We also found that when PHB was replaced with PHB-*g*-AA in the composite, T_m decreased (by about 1–3°C) and ΔH_m increased (by about 8–15 J/g). This is caused by a slight decrease in molecular weight and intrinsic viscosity and a slight increase in melt-flow index in PHB-*g*-AA, due to some degradation of the bond in the grafting reaction. Also of relevance is that the lower melt viscosity of PHB-*g*-AA/WFs compared with PHB/WFs means it could be processed more easily.

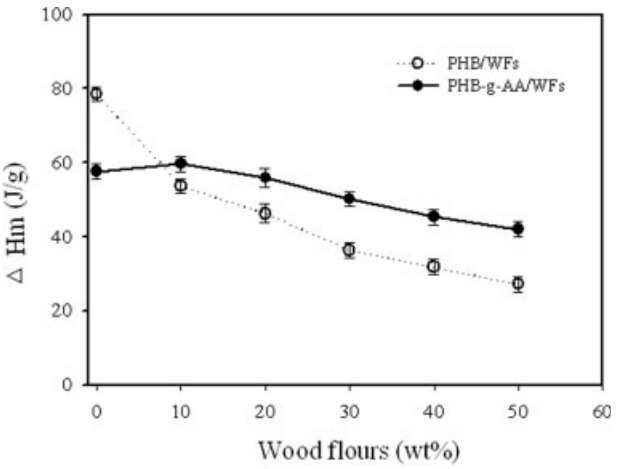

Figure 7 Fusion heat versus WFs content for PHB/WFs and PHB-*g*-AA/WFs blends.

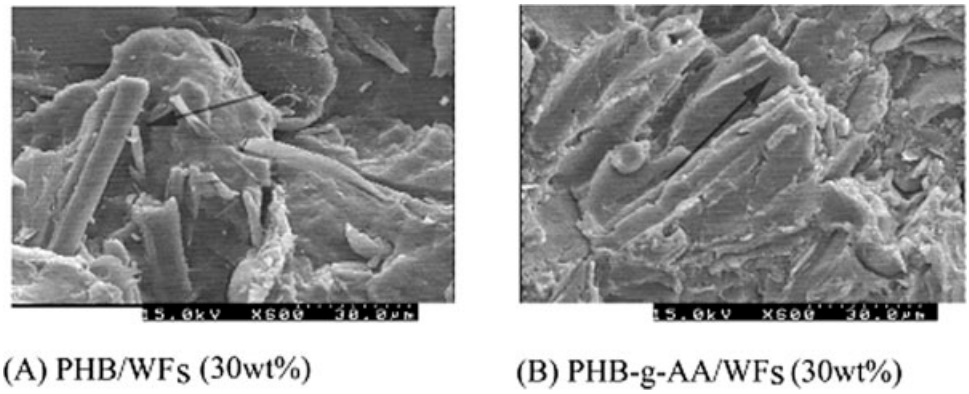

Figure 8 SEM micrographs of PHB/WFs (30 wt %) and PHB-*g*-AA/WFs (30 wt %) blends.

Composite morphology

It is necessary to study the morphology of the polymer blends since the mechanical properties depend on it. For the blends studied in this article, the major component (PHB or PHB-*g*-AA) forms the matrix and the minor component (WFs) is the dispersed phase. In general, good dispersion of WFs in the matrix, effective wetting of WFs by the matrix, and strong interfacial adhesion between the two phases are required to obtain a composite material with satisfactory mechanical properties. Scanning electron microscopy (SEM) was used to study the tensile fracture surfaces of composite samples of PHB/WFs (30 wt %) and PHB-*g*-AA/WFs (30 wt %) blends. The fracture surfaces of PHB/WFs (30 wt %) blend [shown in Fig. 8(A)] indicate that the WFs in this blend tend to agglomerate into bundles and become unevenly distributed throughout the matrix. The poor dispersion of WFs in the PHB matrix is due to the formation of hydrogen bonds and the wide difference in character between PHB and WFs. The markers in Figure 8(A) also show the poor wetting of WFs when PHB/WFs was used. The reason for this is the large difference in surface energy between WFs and the PHB matrix.[8] For the PHB-*g*-AA/WFs (30 wt %) blend there is a better dispersion and homogeneity of WFs in the PHB-*g*-AA matrix. It can be seen from Figure 8(B) that better wetting is obtained since layers of the matrix material have been pulled out together with the WFs over the entire fracture surface. This occurs because of branched and cross-linked macromolecules between WFs surfaces and the PHB-*g*-AA matrix, giving the two components more similar properties and preventing hydrogen bonds from being formed.

Mechanical properties

Figure 9 shows the variation in tensile strength at break with WFs content for PHB/WFs and PHB-*g*-AA/WFs blends. It can be seen that the tensile strength of pure PHB decreased when it was grafted with acrylic acid. For PHB/WFs blends (dotted line in Fig. 9), tensile strength at break decreased markedly and continuously as WFs content was increased, this is due to the poor dispersion of WFs in the PHB matrix, showing that incompatibility between the two polymers has a significant impact on the mechanical properties. The tensile strength of PHB-*g*-AA/WFs (solid line in Fig. 9) is lower than that of PHB. Tensile strength increased at 10% WFs, due to esterification between PHB-*g*-AA and WFs. It subsequently decreased with increasing WFs content, however, due to residual WFs, present because of the low grafting rate of 5.75%, agglomerating and unevenly distributing throughout the matrix. Furthermore, it was found that the PHB-*g*-AA/WFs blends not only gave larger values of tensile strength than the PHB/WFs blends, but that they also provided stable values of tensile strength when the WFs content was above 30 wt %. This may in part be due to the better dispersion, coming from the formation of branched macromolecules of WFs in the PHB-*g*-AA matrix.

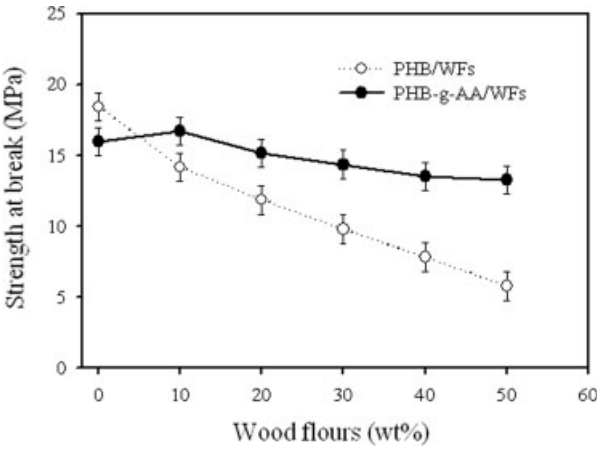

Figure 9 Tensile strength at breakpoint versus WFs content for PHB-*g*-AA and PHB composites. The dotted and solid lines indicate PHB and PHB-*g*-AA, respectively.

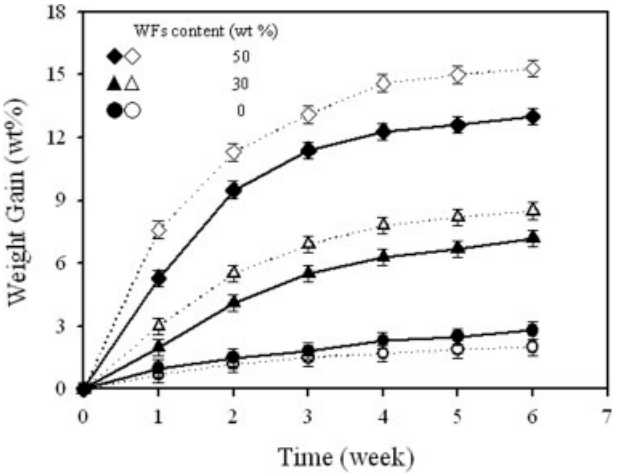

Figure 10 Percentage weight gain of PHB/WFs and PHB-*g*-AA/WFs blends during water absorption. The dotted and solid lines indicate PHB and PHB-*g*-AA, respectively.

It is concluded that the PHB-*g*-AA/WFs blends improved the tensile strength of PHB/WFs. Bikiaris and Panayiotou[26] reported similar outcomes in their analyses of mechanical properties.

Water absorption

The PHB-*g*-AA/WFs blend exhibited moderately good water resistance, higher than that of the PHB/WFs blend at the same WFs content (Fig. 10). The higher water resistance of PHB-*g*-AA/WFs was attributed to the ester carbonyl functional group of that blend. For both blends, the percentage water gain over the 6-week test period increased with WFs content. This was probably due to the increased difficulty in forming polymer chain arrangements with greater amounts of WFs, and to the hydrophilic character of WFs causing poor adhesion with the hydrophobic PHB or PHB-*g*-AA. Oksman and Clemons[17] present similar findings in their study of blends of WFs and polyethylene. The water gain shown by PHB is lower than that of PHB-*g*-AA, owing to the more hydrophilic nature of PHB-*g*-AA.

Biodegradation under enzymatic environment

Exposure to soil environment

Figure 11 shows changes in weight ratio (degraded sample/initial sample) with time for the PHB/WFs and PHB-*g*-AA/WFs buried in soil. In the soil, water diffused into the polymer sample, causing swelling and enhancing biodegradation. The blends containing higher percentages of WFs (30 and 50%) degraded rapidly in the initial 6 weeks, equivalent to the approximate WFs content of the blends, and a gradual decrease of weight occurred during the next 6 weeks.

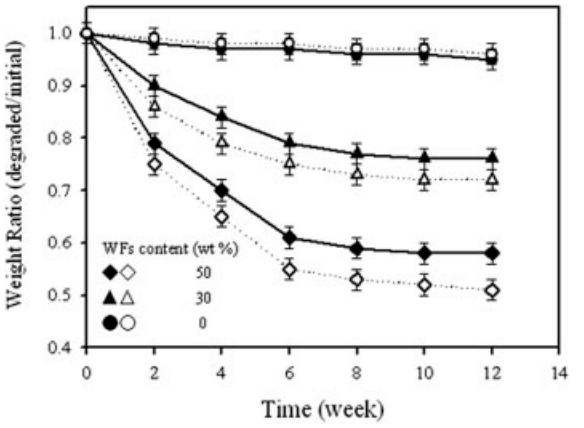

Figure 11 Weight ratio of PHB/WFs and PHB-*g*-AA/WFs blends exposed to soil environment. The dotted and solid lines indicate PHB and PHB-*g*-AA, respectively.

The weight loss of WFs, which indicated the extent of biodegradation of the blends, both increased as the content of WFs increased. Further comparison of the two copolymers revealed that PHB-*g*-AA/WFs had a higher weight ratio, with an increment of about 0.02–0.10. The greater biodegradation of PHB/WFs may be caused by the same factors leading to its higher absorption of water. Under the soil environment, the mechanical properties of blends, such as tensile strength, also deteriorated.

Exposure to enzymatic environment

Although it takes longer time than that in a soil environment, PHB can be degraded into CO_2, H_2O, and some nontoxic compounds under an enzymatic environment, with a concomitant reduction in mechanical properties. Figure 12 shows changes in weight ratio (degraded sample/initial sample) with

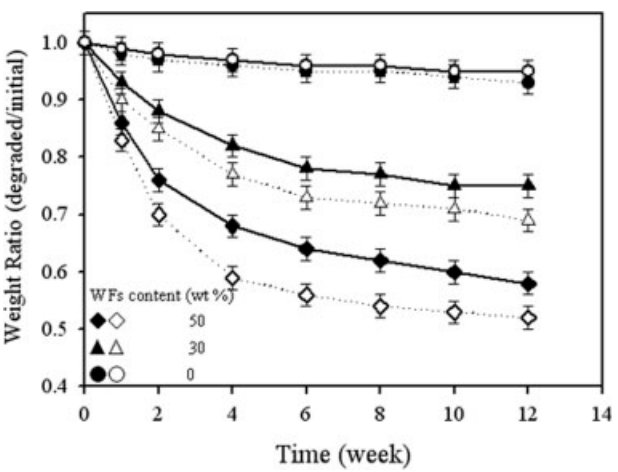

Figure 12 Weight ratio of PHB/WFs and PHB-*g*-AA/WFs blends exposed to enzymatic environment. The dotted and solid lines indicate PHB/WFs and PHB-*g*-AA/WFs, respectively.

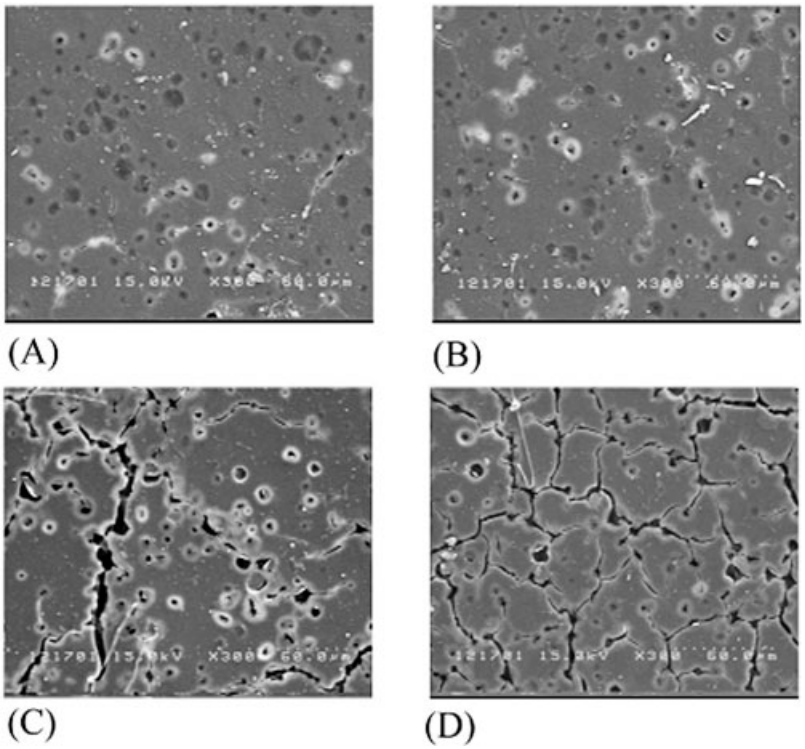

Figure 13 SEM micrographs of PHB-*g*-AA/WFs (30 wt %) exposed to enzymatic environment. (A): 1 week; (B): 2 weeks; (C): 4 weeks; (D): 6 weeks.

time for the PHB/WFs and PHB-*g*-AA/WFs incubated with α-amylase. The rate of degradation was affected by blending with WFs in a similar way to degradation in a soil environment, and for similar reasons.

Morphological analysis provided further illustration of the variation in biodegradation of PHB-*g*-AA over time, and showed that the modified composite deteriorated severely over time (shown in Fig. 13). Indeed, after 6 weeks the modified composite was almost cracked. Thereafter, degradation continued while the rate leveled off.

CONCLUSIONS

Using PHB-*g*-AA in place of PHB in a PHB/WFs composite improved the compatibility and mechanical properties of the composite. The crystalline structure of PHB-*g*-AA/WFs differs from that of PHB/WFs, due to the formation of an ester carbonyl functional group from the reaction between the —OH of WFs and the —COOH of PHB-*g*-AA. For both composites, both the melting temperature(T_m) and fusion heat (ΔH_m) decrease with increasing WFs content. The PHB-*g*-AA/WFs blends were more easily processed due to their lower melt temperatures and torque values. Investigation of the morphology of PHB-*g*-AA/WFs confirmed a good adhesion between WFs and the PHB-*g*-AA matrix. Mechanical testing demonstrated that the use of PHB-*g*-AA, as opposed to PHB, enhanced the mechanical properties of the blends, especially tensile strength. We conclude that the PHB-*g*-AA copolymer produced in our laboratory can be used to lower the cost and to improve the properties of PHB/WFs type blends. Although water resistance of PHB-*g*-AA/WFs was higher than that of PHB/WFs, the compatibilized blend showed only a slightly lower biodegradation rate than the uncompatibilized blend when exposed to soil and enzymatic environments.

References

1. Kim, M. N.; Lee, A. R.; Lee, K. H.; Chin, I. J.; Yoon, J. S. Eur Polym J 1999, 35, 1153.
2. Borkenhagen, M.; Stoll, R. C.; Neuenschwander, P.; Suter, U. W.; Aebischer P. Biomaterials 1998, 19, 2155.
3. Wu, C. S. Macromol Biosci 2005, 5, 352.
4. Simonsen, J.; Jacobsen, R.; Rowell, R. J Appl Polym Sci 1998, 68, 1567.
5. Wu, C. S. J Appl Polym Sci 2003, 89, 2888.
6. Oksman, K.; Lindberg, H.; Holmgren, A. J Appl Polym Sci 1998, 69, 201.
7. Oksman, K.; Lindberg, H. J Appl Polym Sci 1998, 68, 1845.
8. Felix, J. M.; Gatenholm, P. J Appl Polym Sci 1991, 42, 609.
9. Wu, C. S.; Hsin-Tzu, L. J Appl Polym Sci 2002, 86, 1792.
10. Gaylord, N. G.; Mehta, R.; Kumar, V.; Tazi, M. J Appl Polym Sci, 1989, 38, 359.
11. Wu, C. S. J Polym Sci Part A: Polym Chem 2003, 41, 3882.
12. Ni, M.; Wang, M. C. Mater Sci Eng 2002, 20, 101.

13. Jedlinski, Z.; Kowalczuk, M.; Adamus, G.; Sikorska, W.; Rydz, J. J Int Biol Macromol 1999, 25, 247.
14. Wu, C. S.; Liao, S. M.; Laio, H. T. J Appl Polym Sci 2002, 85, 2905.
15. Kim, J.; Tirrell, D. A. Macromolecules 1999, 32, 945.
16. Liao, H.-T.; Wu, C. S. J Appl Polym Sci 2003, 88, 1919.
17. Oksman, K.; Clemons, C. J Appl Polym Sci 1998, 67, 1503.
18. Doi, Y.; Kunioka, M.; Nakamura, Y.; Soga, K. Macromolecules 1988, 21, 2722.
19. Maunu, S. L. Prog Nucl Magn Reson Spectrosc 2002, 40, 151.
20. Galego, N.; Rozsa, C.; Sanchez, R.; Fung, J.; Vazquez, A.; Tomas, J. S. Polym Test 2000, 19, 485.
21. Nunez, A. J.; Kenny, J. M.; Reboredo, M. M.; Aranguren, M. I.; Marcovich, N. E. Polym Eng Sci 2002, 42, 733.
22. Arvanitoyannis, I.; Biliaderis, C. G.; Ogawa, H.; Kawasaki, N. Carbohydr Polym 1998, 36, 89.
23. Shogren, R. L.; Thompson, A. R.; Felker, F. C.; Harry-Okuru, R. E.; Gordon, S. H.; Greeen, R. V.; Gould, J. M. J Appl Polym Sci. 1992, 44, 1971.
24. Aburto, J.; Thiebaud, S.; Alric, I.; Bikiaris, D.; Prinos, J.; Panayioyou, C. Carbohydr Polym 1997, 34, 101.
25. Averous, L.; Moro, L.; Fringant, C. Polymer 2000, 41, 4157.
26. Bikiaris, D.; Panayiotou, C. J Appl Polym Sci 1998, 70, 1503.